

Preliminary CHIME dating of granites from the Nkambe area, northwestern Cameroon, Africa

Samuel TETSOPGANG, Kazuhiro SUZUKI and Mamoru ADACHI

*Department of Earth and Planetary Sciences, Graduate School of Science,
Nagoya University, Nagoya 464-8602, Japan*

(Received October 29, 1999 / Accepted November 24, 1999)

ABSTRACT

The chemical Th-U-total Pb isochron method (CHIME) has been adopted for dating the syntectonic foliated and post-tectonic unfoliated granites in northwestern Cameroon. The CHIME ages are 532 ± 35 Ma for allanite and 523 ± 45 Ma for zircon from Sample I₁₀ of foliated biotite granite, 530 ± 9 Ma for monazite from Sample N₉ of foliated two-mica granite, and 510 ± 25 Ma for monazite from Sample I₄ of unfoliated two-mica granite. Several monazite grains from Sample N₉ and I₄ yield 436 ± 13 and 420 ± 16 Ma CHIME ages, respectively. The 532-510 Ma ages are interpreted as the time of granite emplacement and the 436-420 Ma ages as the time of hydrothermal alteration. The CHIME ages coupled with the concordant relation between the foliated granites and migmatitic gneiss suggest a ca. 530 Ma metamorphic-plutonic episode in northwestern Cameroon rather than a thermal overprint by granite intrusion.

INTRODUCTION

The Pan-African orogeny was recorded in a wide area of Africa (Kröner, 1977), but the timing and nature of individual mobile zones have remained unclear. The main point of argument is whether the numerous Cambrian (ca. 530 Ma) ages record a single cycle with integral sedimentary-metamorphic-plutonic episodes or a simple thermal imprint on older rocks through granite intrusion. Tingey (1991) regarded the 500 Ma event in East Gondwana as a thermal event free from deformation. Recent geochronological studies, however, have disclosed a widespread occurrence of Cambrian granulite-facies paragneisses in East Antarctica ($521-553$ Ma, Shiraishi et al., 1994; $529\pm 14 - 541\pm 15$ Ma, Asami et al., 1996, 1997), South India (527 ± 10 Ma, Bindu et al., 1998) and Madagascar ($527\pm 15 - 534\pm 10$ Ma, Ito et al., 1997). Since the paragneisses contain 622-797 Ma detrital monazites (Asami et al., 1997; Ito et al., 1997) and 640-800 Ma detrital zircons (Shiraishi et al., 1994, Bindu et al., 1996), they do not represent reworked older basements, but formed newly from post-620 Ma sediments by the single metamorphism linked to the collision of East Gondwana (Shiraishi et al., 1994; Asami et al., 1997; Ito et al., 1997). West Gondwana, on the other hand, has been considered to have formed by the collision of the Western Africa craton, Congo craton and a Proterozoic mobile zone during the Pan-African-Brasiliano orogeny (Castaing et al., 1993; Trompette, 1994). The timing of the metamorphism and plutonism during the Pan-African-Brasiliano orogeny is important for proper understanding of the amalgamation history of the Gondwana supercontinent. Cameroon, located to the north of

the Congo craton (Fig. 1: e.g. Kennedy, 1964; Rocci, 1965; Clifford, 1970), occupies a key position for studying of the Pan-African-Brasiliano orogeny.

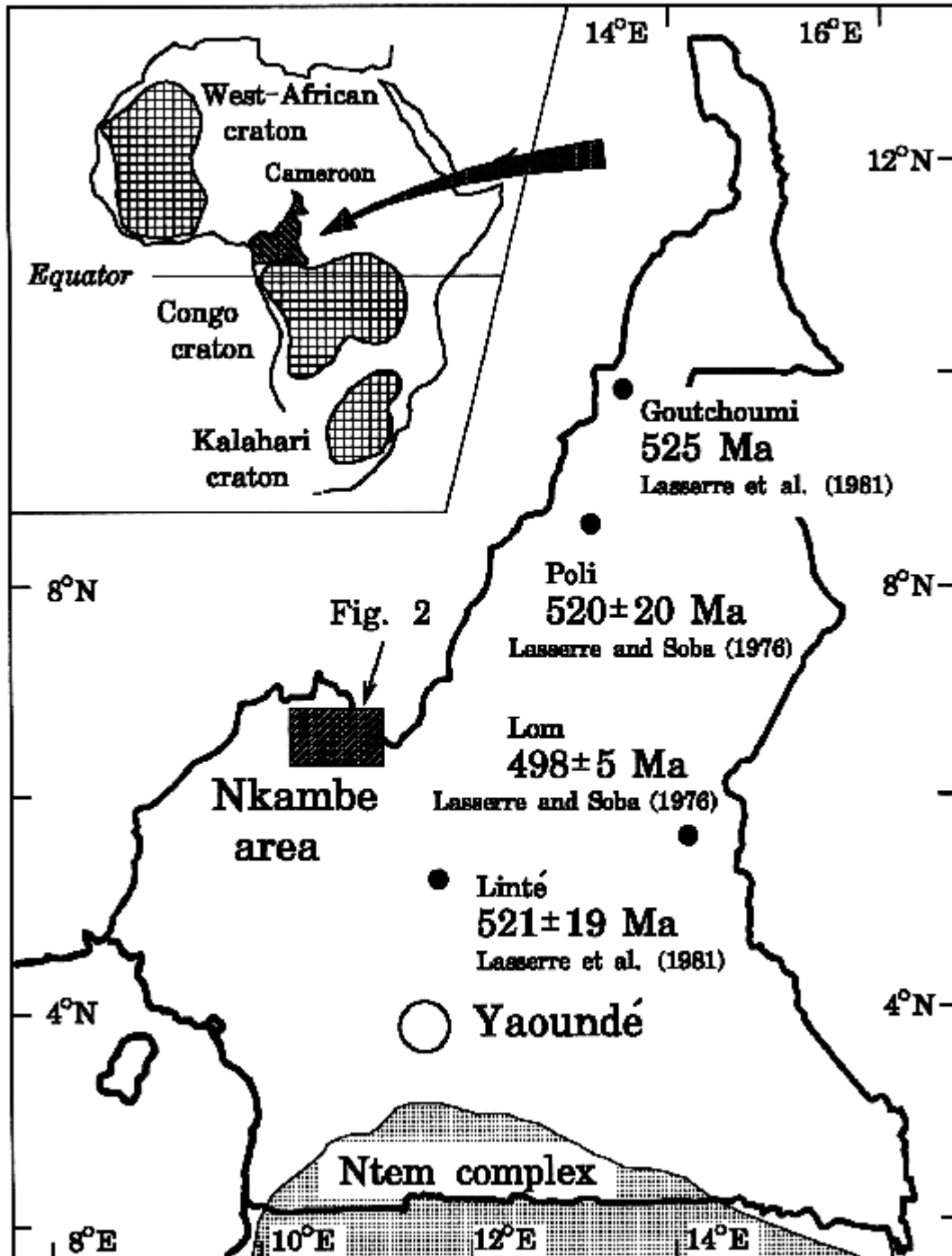


Fig. 1. Map showing the location of the Nkambe area in northwestern Cameroon. The location of the Ntem Complex of the Congo craton and radiometric ages reported by Lasserre and Soba (1976) and Lasserre et al. (1981) are also shown. Inset map shows the distribution of craton in Africa (after Kennedy, 1964).

Lasserre (1966) separated the basement rocks in Cameroon into the Ntem Complex in the southern end of Cameroon and the Central-Africa mobile zone in the rest of the territory. The Ntem Complex constitutes the northern part of the Congo craton, and consists predominantly of charnockitic gneiss and granites. Studies on the Ebolowa Granite have yielded 2.5 and 3.2 Ga Pb-a zircon ages (Cahen and Snelling, 1966), a 2566 ± 100 Ma K-Ar hornblende age (Lasserre, 1969) and a 3010 ± 50 Ma Rb-Sr whole-rock isochron age (Lasserre and Bessoles, 1976). Other granitoids have Rb-Sr biotite ages of 1800-2350 Ma (Cahen and Snelling, 1966; Lasserre, 1969).

The Central-Africa mobile zone is composed of a mixture of schist, gneiss, migmatite and granite. Granitic rocks in the mobile zone have been classified into two groups, "uncircumscribed" granites with a marked foliation and/or mylonitic texture and "circumscribed" granites with no foliation (Bessoles and Trompette, 1980). Hereafter, we designate the uncircumscribed and circumscribed granite as the foliated and unfoliated granites, respectively. The foliated granite was emplaced possibly during the Pan-African orogeny and the unfoliated one on an later anorogenic stage. Rb-Sr age data have been reported for granitoids from Groutchoumi (ca. 525 Ma, Lasserre et al., 1981), Poli (520 ± 20 Ma, Lasserre and Soba, 1976), Linté (521 ± 19 Ma, Lasserre et al., 1981), and Lom (498 ± 5 Ma, Lasserre and Soba, 1976). We, however, are not confident whether these ages date the intrusion time of the foliated granite or the overprint time by the intrusion of the unfoliated granite.

The Nkambe area in northwestern Cameroon (Fig. 1) is underlain by predominantly granitic rocks. These granitoids, like those in other area of the Central-African mobile zone, can be classified into the foliated and unfoliated types. CHIME dating by the authors is currently in progress, to know the emplacement ages of the granitoids. This paper reports CHIME age data for representative samples of the foliated and unfoliated granites from the Nkambe area.

GEOLOGICAL OUTLINE AND SAMPLE DESCRIPTION

The Nkambe area ranges in latitude from $6^{\circ}25'$ to $6^{\circ}53'$ N and in longitude from $10^{\circ}22'$ to $11^{\circ}00'E$ (Fig. 1). The area consists mainly of plateaus with deep river valleys flowing in to the Donga River in the northeast, and high volcanic mountains in the southeast. The geology of the Nkambe area is shown in Fig. 2. The basement rocks include magmatitic gneiss, anatectic granite, amphibolite and granite, which are overlain in part by Cenozoic basalt, andesite and alkali rhyolite (Peronne, 1969). The migmatitic gneiss trends NNE-SSW direction.

Granitic rocks in the Nkambe area consist of the foliated and unfoliated granites. Although these types are not distinguished in the map, the former type includes biotite granite, anatectic granite and small phacoliths in the migmatitic gneiss domains in Fig. 2. Since the foliated granites grade into the migmatitic gneiss at the margins and are deformed along with the migmatitic gneiss, they can be regarded as syntectonic intrusives. The unfoliated granites intrude into the migmatitic gneiss as small stocks of about 500-1000 m in diameter.

Two samples (Sample I₁₀ and N₉) of the foliated granite and one sample (Sample I₄) of the unfoliated granite were used for the present CHIME dating. The sample

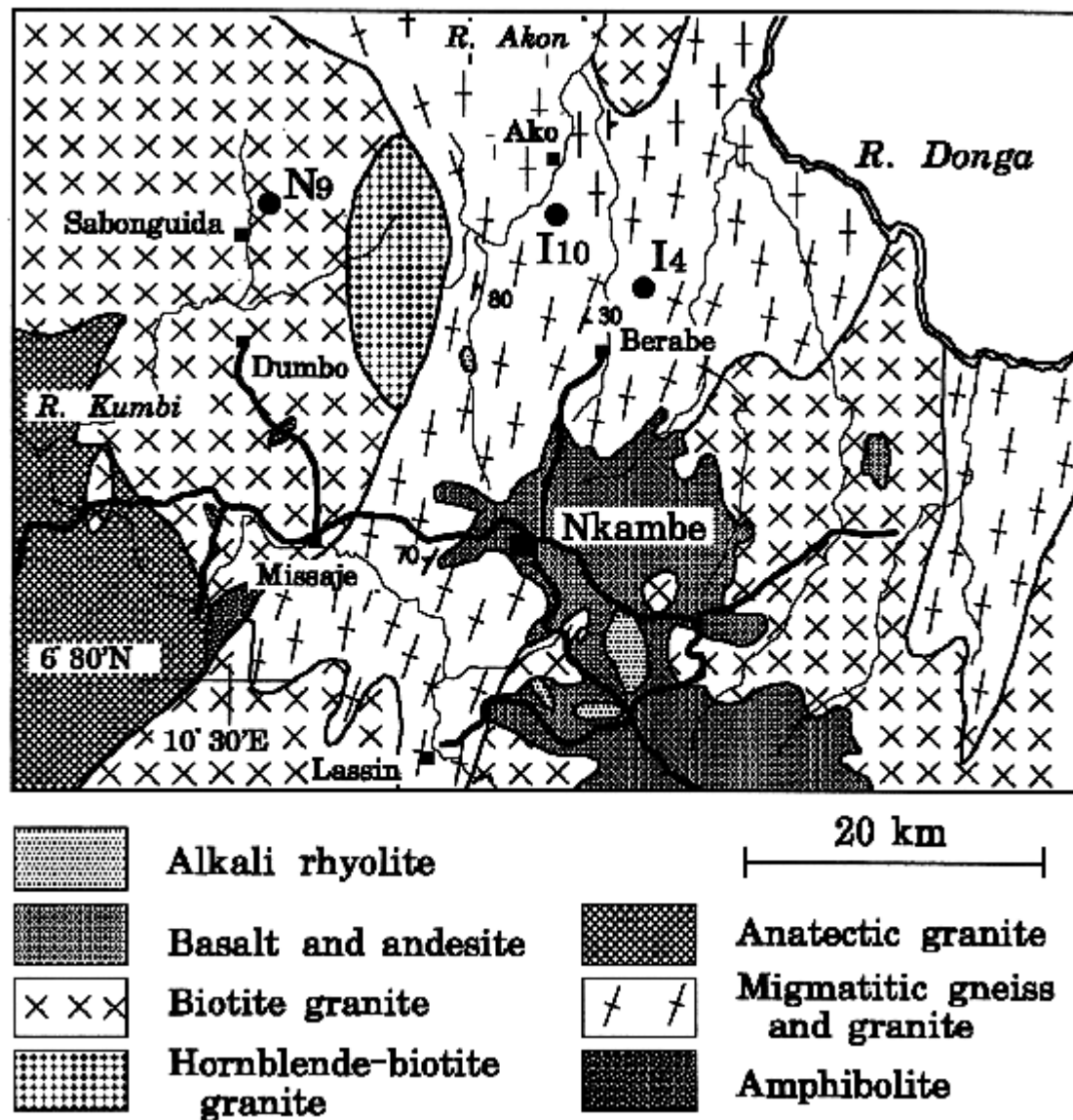


Fig. 2. Geological map of the Nkambe area (simplified and modified from Peronne, 1969). Sample localities are indicated by solid circles.

localities are shown in Fig. 2.

Sample I₁₀ was collected from a phacolith in the migmatitic gneiss domain. It is of biotite granite containing quartz, microcline, plagioclase, biotite and muscovite. The modal proportions of quartz, microcline and plagioclase are 41.2, 49.4 and 9.4%, respectively. Quartz porphyroclasts exhibit a strong wavy extinction, and are granulated along their grain boundaries. Feldspar porphyroclasts are extensively deformed. Granulated particles are flattened, and form a fine-grained matrix. Biotite and muscovite flakes are commonly kinked. Accessory minerals include zircon, allanite and magnetite. Zircon occurs as euhedral prisms of 0.1 to 0.3 mm in length. No visible cores or overgrowth rims can be observed, but some grains show concentric growth zoning. Allanite occurs as inclusions in deformed quartz porphyroclasts as well as in

deformed biotite flakes.

Sample N₉, a medium-grained porphyritic two-mica granite, was collected from the central part of the concordant biotite granite domain in Fig. 2. It is foliated and consists mainly of quartz, microcline-microperthite, plagioclase, biotite and muscovite. Myrmekites of quartz and feldspar are common. The modal proportions of quartz, microcline and plagioclase are 31.2, 39.6 and 29.2%, respectively. Quartz grains are granulated along their boundaries. Feldspar grains remain resistant to granulation, and are responsible for the porphyritic texture. Biotite flakes are not deformed, and in some place are replaced by chlorite. Accessory minerals include apatite, zircon, monazite and magnetite. Zircon occurs as transparent euhedral prismatic crystals of 0.1-0.2 mm in length, and is found in quartz and microcline, and along grain boundaries. Subhedral to anhedral grains of monazite, up to 0.2 mm across, occur on the boundaries of quartz and feldspar grains, and are also found within the foliated matrix. Most monazite grains are inclusion-free, although several anhedral monazite grains contain minute black inclusions.

Sample I₄ is undeformed fine-grained two-mica adamellite with magnetite grains 2-5 mm across. It consists mainly of quartz, sodic oligoclase, microcline, biotite and muscovite. The modal proportions of quartz, microcline and plagioclase are 31.2, 32.9 and 35.9%, respectively. Biotite is almost entirely altered to chlorite. Some muscovite is intergrown with biotite. Magnetite grains are surrounded by pink-colored altered patches 5-10 mm across. Under the microscope, the magnetite grains are fringed with secondary muscovite, and feldspars in the altered patches are replaced partly by an aggregate of muscovite. Accessory minerals include monazite, zircon and apatite. Monazite grains are more abundant than zircon, and range from 0.1 to 0.4 mm across. Monazite grains in the fresh part of the sample are clear, but those in the altered patches are studded with minute black inclusions and are altered at the margin to apatite and an unidentified REE-, Fe- and Ca-bearing brown to opaque mineral.

CHIME DATING

Monazite, allanite and zircon were analyzed on a JEOL JCXA-733 electron microprobe equipped with four wavelength-dispersive type spectrometers. The details of sample preparation and analysis have been described elsewhere (Suzuki and Adachi, 1991a, b; Suzuki et al., 1999). The detection limit of ThO₂, UO₂ and PbO at a 2 σ confidence level are 0.015, 0.02 and 0.006%, respectively. The relative errors in the PbO determination are 30, 10, 5 and 3% at -0.02, -0.1, -0.2 and 0.4 wt. % levels, respectively. The relative errors in the ThO₂ and UO₂ determinations are 20, 10, 5, 3 and 1% at <0.1, -0.3, -4 and >8 wt.%, respectively. The ThO₂, UO₂ and PbO analytical results are listed in Table 1. CHIME ages were calculated as described by Suzuki and Adachi (1991a, b, 1994, 1998) and Suzuki et al. (1991, 1994, 1999).

Sample I₁₀: biotite granite

A total of 39 spots on 7 allanite grains and 9 spots on 2 zircon grains were analyzed. The ThO₂ concentration in allanite ranges from 1.32 to 12.3%, UO₂ from 0.039 to 1.61%, and PbO from 0.036 to 0.224%. Thirty-one of the 39 analyses form a linear array on the PbO-ThO₂* diagram (Fig. 3A), with the rest of the analyses plotted below the array.

Table 1. Electron microprobe analyses (wt.%) of ThO₂, UO₂ and PbO of allanite (A), zircon (Z) and monazite (M) from foliated (Samples I₁₀ and N₉) and unfoliated (Sample I4) granites in northwestern Cameroon. Age: apparent age in Ma, RO₂*: (ThO₂*) measured ThO₂ plus ThO₂ equivalent of the measured UO₂ for allanite and monazite and (UO₂*) measured UO₂ plus UO₂ equivalent of the measured ThO₂ for zircon.

Spot No.	ThO ₂	UO ₂	PbO	Age	RO ₂ *	Spot No.	ThO ₂	UO ₂	PbO	Age	RO ₂ *
Sample I ₁₀ (foliated granite)						Sample N ₉ (foliated granite)					
A01-01 *	3.85	0.062	0.103	594	4.06	M01-01 /	7.82	0.335	0.173	457	8.93
A01-02 *	3.13	0.049	0.0782	557	3.30	M01-02 *	14.5	0.588	0.363	519	16.5
A01-03 *	5.00	0.072	0.127	569	5.23	M01-03	11.2	0.441	0.266	494	12.7
A01-04	6.85	0.122	0.128	414	7.25	M01-04	8.39	0.369	0.198	485	9.61
A01-05	12.3	0.171	0.105	193	12.9	M01-05 *	16.2	0.548	0.397	516	18.1
A01-06 *	3.61	0.049	0.0847	528	3.77	M01-06 *	16.5	0.549	0.408	524	18.3
A01-07 *	3.87	0.109	0.101	558	4.23	M01-07 *	15.1	0.479	0.367	516	16.7
A01-08 *	3.40	0.059	0.0934	608	3.60	M01-08	11.3	0.386	0.266	498	12.6
A01-09 *	7.74	0.126	0.168	484	8.16	M01-09	9.73	0.374	0.232	496	11.0
A01-10	10.5	0.153	0.108	233	11.0	M01-10 *	7.48	0.327	0.184	504	8.56
A01-11	7.35	0.111	0.130	396	7.72	M01-11	8.64	0.299	0.199	487	9.62
A01-12	3.40	0.089	0.0369	237	3.69	M01-12	12.2	0.387	0.281	489	13.5
A02-01	2.59	0.671	0.0505	250	4.77	M01-13 /	7.95	0.403	0.182	462	9.28
A02-02 *	4.26	1.61	0.224	549	9.60	M01-14 *	21.0	0.605	0.518	529	23.0
A02-03 *	4.00	0.306	0.112	525	5.01	M01-15 /	16.8	0.334	0.315	415	17.9
A02-04 *	3.44	0.605	0.145	623	5.45	M01-16 /	5.03	0.277	0.111	440	5.94
A03-01 *	2.92	0.154	0.0777	533	3.42	M02-01	9.55	0.374	0.220	480	10.8
A03-02 *	3.46	0.448	0.112	530	4.95	M02-02 *	7.20	0.333	0.179	507	8.30
A03-03	2.47	0.906	0.0486	213	5.40	M02-03	7.99	0.364	0.191	488	9.19
A03-04 *	1.83	0.103	0.0602	648	2.18	M02-04	8.14	0.390	0.197	490	9.43
A03-05 *	3.64	0.424	0.123	572	5.04	M02-05	6.40	0.326	0.156	490	7.48
A03-06 *	3.94	0.737	0.1273	470	6.37	M02-06 *	5.90	0.323	0.151	510	6.97
A03-07	3.39	1.04	0.120	415	6.81	M02-07	9.53	0.460	0.229	487	11.0
A04-01 *	1.32	0.039	0.0361	584	1.45	M02-08 /	7.57	0.393	0.172	455	8.87
A04-02 *	3.97	1.27	0.202	577	8.20	M02-09 *	8.39	0.411	0.213	513	9.75
A04-03 *	4.87	0.107	0.125	563	5.22	M02-10 *	9.11	0.403	0.227	510	10.4
A05-01 *	3.09	0.057	0.0837	599	3.28	M02-11 /	7.70	0.384	0.170	447	8.96
A05-02 *	3.17	0.065	0.0801	556	3.38	M02-12 *	5.95	0.320	0.150	504	7.01
A05-03 *	3.70	0.073	0.0980	583	3.94	M02-13	8.66	0.359	0.203	485	9.85
A05-04 *	3.61	0.069	0.0950	580	3.84	M02-14	7.73	0.436	0.191	491	9.17
A05-05 *	3.71	0.057	0.0869	523	3.90	M02-15 *	7.95	0.417	0.208	523	9.33
A05-06 *	3.30	0.062	0.0757	507	3.51	M02-16	7.33	0.377	0.179	489	8.58
A06-01 *	5.10	0.104	0.124	533	5.45	M02-17	6.21	0.333	0.151	486	7.31
A06-02 *	4.20	0.075	0.106	558	4.45	M02-18	7.03	0.331	0.168	488	8.12
A07-01 *	2.81	0.060	0.0655	512	3.01	M02-19 /	11.4	0.349	0.242	454	12.5
A07-02 *	3.25	0.074	0.0840	565	3.49	M02-20 *	5.85	0.374	0.153	506	7.09
A07-03 *	2.77	0.061	0.0673	532	2.97	M03-01 /	8.15	0.455	0.187	457	9.65
A07-04 *	3.47	0.063	0.0833	531	3.68	M03-02	8.01	0.409	0.186	467	9.36
A07-05 *	3.34	0.052	0.0762	509	3.52	M03-03 /	8.70	0.371	0.190	450	9.92
A07-06	4.01	0.083	0.0777	427	4.28	M03-04 /	18.9	0.611	0.393	443	20.9
Z01-01 *	0.230	0.261	0.0244	528	0.330	M03-05	7.62	0.408	0.184	482	8.97
Z01-02 *	0.238	0.254	0.0243	533	0.326	M03-06 /	7.59	0.377	0.160	428	8.83
Z01-03 *	0.260	0.279	0.0279	557	0.357	M03-07 /	9.63	0.409	0.203	435	11.0
Z01-04 *	0.187	0.255	0.0232	533	0.312	M03-08 /	7.77	0.456	0.178	453	9.27
Z01-05 *	0.111	0.170	0.0163	572	0.203	M03-09 /	7.90	0.446	0.170	426	9.37
Z01-06 *	0.270	0.279	0.0214	428	0.362	M03-10 /	7.25	0.419	0.151	412	8.63
Z02-01 *	0.061	0.185	0.0166	582	0.203	M04-01 /	7.29	0.468	0.165	441	8.83
Z02-02 *	0.087	0.121	0.0113	548	0.147	M04-02 /	6.76	0.434	0.153	438	8.19
Z02-03 *	0.099	0.208	0.0173	521	0.238	M04-03 /	6.69	0.433	0.149	432	8.12
						M04-04 /	7.10	0.465	0.159	433	8.63
						M04-05 /	7.40	0.324	0.162	450	8.46
						M04-06 /	10.2	0.438	0.218	441	11.6
						M04-07 /	7.82	0.344	0.170	447	8.95
						M05-01 /	8.34	0.506	0.189	444	10.0
						M05-02	7.89	0.473	0.200	497	9.45
						M05-03 *	7.62	0.472	0.201	513	9.18
						M05-04	8.27	0.501	0.210	497	9.92
						M05-05	7.79	0.477	0.199	499	9.36

* marks data points shown with solid circles in Figs. 3, 4 and 5, and / marks data points shown with open circles

Table 1. (continued)

Spot No.	ThO ₂	UO ₂	PbO	Age	RO ₂ *	Spot No.	ThO ₂	UO ₂	PbO	Age	RO ₂ *
M05-06 *	5.13	0.324	0.137	517	6.20	M10-29	6.87	0.266	0.168	508	7.76
M05-07	7.85	0.453	0.194	487	9.34	M10-30	8.87	0.412	0.201	463	10.2
M05-08 *	8.27	0.455	0.213	513	9.78	M10-31	9.94	0.525	0.232	468	11.7
M05-09 *	6.58	0.400	0.171	507	7.91	M10-32 *	6.90	0.279	0.168	504	7.83
M05-10 *	5.14	0.338	0.138	518	6.26	M10-33 *	10.3	0.404	0.248	502	11.6
M05-11 *	8.23	0.444	0.207	502	9.70	M10-34 *	7.61	0.328	0.194	523	8.70
M05-12	8.21	0.449	0.205	497	9.70	M10-35 *	6.71	0.342	0.169	507	7.84
M05-13 *	5.59	0.356	0.144	500	6.76	M10-36 *	6.71	0.285	0.165	506	7.65
M05-14	8.01	0.428	0.194	485	9.42	M10-37 *	7.73	0.358	0.201	529	8.92
M05-15	6.53	0.415	0.158	472	7.89	M10-38 *	6.62	0.300	0.163	502	7.61
M05-16	6.50	0.282	0.146	461	7.43	M10-39	7.20	0.323	0.173	491	8.27
M05-17 /	6.53	0.267	0.143	454	7.41	M10-40 *	6.40	0.240	0.155	505	7.19
M05-18	6.52	0.340	0.156	479	7.64	M10-41 *	7.37	0.330	0.188	522	8.47
M05-19 /	9.04	0.321	0.193	449	10.1	M10-42 *	8.23	0.378	0.211	521	9.49
M05-20 /	5.43	0.270	0.122	454	6.32	M10-43 *	5.66	0.256	0.147	531	6.51
M06-01 /	9.63	0.298	0.201	445	10.6	M10-44 *	8.29	0.357	0.212	526	9.47
M06-02 /	11.3	0.341	0.242	459	12.4	M10-45 *	7.69	0.320	0.192	516	8.75
M06-03 /	11.6	0.369	0.237	436	12.8	M10-46 *	5.99	0.344	0.153	504	7.13
M06-04 /	9.98	0.242	0.203	444	10.8	M10-47 *	10.2	0.391	0.258	526	11.5
M06-05 /	11.2	0.335	0.234	449	12.3	M10-48 *	6.02	0.335	0.150	495	7.13
M07-01 /	9.73	0.295	0.200	439	10.7	M10-49 *	9.09	0.373	0.225	513	10.3
M07-02 /	10.2	0.329	0.215	451	11.2	M10-50 *	4.01	0.239	0.103	503	4.80
M07-03	9.92	0.322	0.216	463	11.0	M10-51	9.14	0.366	0.218	496	10.3
M07-04	8.34	0.267	0.187	477	9.22	M10-52 *	7.38	0.337	0.185	511	8.49
M07-05	9.76	0.319	0.214	466	10.8	M10-53 *	6.40	0.382	0.167	511	7.66
M08-01 /	10.3	0.203	0.211	451	11.0	M10-54 *	7.46	0.383	0.196	528	8.73
M08-02	9.80	0.207	0.210	470	10.5	M10-55 *	10.7	0.458	0.282	544	12.2
M08-03 /	10.5	0.231	0.214	445	11.3	M10-56 *	7.06	0.277	0.178	525	7.98
M08-04 /	11.5	0.316	0.243	454	12.6	M10-57 *	7.31	0.309	0.187	528	8.33
M08-05 /	10.5	0.200	0.215	453	11.1	M10-58 *	6.94	0.319	0.185	544	7.99
M09-01	8.18	0.187	0.176	471	8.79	M10-59 *	6.91	0.249	0.178	540	7.74
M09-02 /	9.21	0.203	0.192	456	9.88	M10-60 *	6.68	0.309	0.181	551	7.70
M09-03	8.66	0.160	0.134	343	9.18	M10-61 *	7.71	0.368	0.208	545	8.93
M09-04 /	8.92	0.207	0.180	440	9.60	M10-62 *	6.54	0.322	0.174	537	7.61
M09-05 /	8.24	0.191	0.172	456	8.87	M10-63 *	7.17	0.343	0.197	555	8.31
M10-01 *	6.26	0.342	0.158	502	7.39	M11-01 *	6.05	0.329	0.156	515	7.14
M10-02 *	6.26	0.344	0.161	512	7.40	M11-02	5.81	0.346	0.147	498	6.96
M10-03 *	5.69	0.322	0.149	517	6.76	M11-03 *	5.82	0.378	0.160	532	7.08
M10-04 *	6.86	0.282	0.178	536	7.79	M11-04 *	6.01	0.273	0.157	532	6.92
M10-05 /	7.70	0.320	0.164	440	8.75	M11-05 *	6.60	0.341	0.173	527	7.72
M10-06 *	6.89	0.317	0.175	518	7.94	M11-06 *	5.87	0.359	0.160	531	7.05
M10-07 *	6.19	0.333	0.157	506	7.29	M11-07 *	5.07	0.323	0.134	514	6.13
M10-08 *	5.84	0.359	0.159	532	7.03	M11-08 *	7.41	0.355	0.199	543	8.58
M10-09 *	8.69	0.347	0.209	500	9.83	M11-09	6.84	0.352	0.170	498	8.00
M10-10 *	7.00	0.326	0.178	517	8.08	M11-10 /	6.08	0.372	0.133	429	7.30
M10-11 *	6.44	0.306	0.159	502	7.45	M11-11 *	6.67	0.338	0.170	512	7.78
M10-12 *	8.72	0.393	0.221	517	10.0	M11-12	7.02	0.341	0.169	488	8.14
M10-13 *	4.33	0.239	0.114	524	5.12	M11-13 /	5.13	0.299	0.117	451	6.11
M10-14 /	6.82	0.318	0.153	457	7.87	M11-14 *	6.00	0.350	0.159	523	7.16
M10-15	5.94	0.357	0.142	469	7.12	M11-15 /	7.49	0.347	0.169	459	8.64
M10-16 *	5.38	0.327	0.145	528	6.46	M12-01 *	6.68	0.394	0.178	524	7.99
M10-17 *	6.95	0.292	0.170	504	7.91	M12-02 /	10.0	0.411	0.202	418	11.4
M10-18 /	7.40	0.366	0.167	456	8.60	M12-03 *	9.88	0.478	0.260	532	11.5
M10-19 *	5.45	0.293	0.141	516	6.42	M12-04 *	8.31	0.297	0.205	518	9.29
M10-20 *	6.74	0.320	0.173	522	7.80	M12-05 *	5.16	0.275	0.133	515	6.07
M10-21 *	9.35	0.388	0.229	507	10.6	M12-06 *	7.99	0.351	0.199	511	9.15
M10-22 *	10.3	0.405	0.265	533	11.7	M12-07 *	9.31	0.432	0.243	530	10.7
M10-23	7.53	0.339	0.170	461	8.65	M12-08 *	9.48	0.425	0.246	531	10.9
M10-24 *	6.87	0.309	0.172	512	7.89	M12-09 *	8.33	0.346	0.213	528	9.48
M10-25 *	5.68	0.318	0.145	505	6.73	M12-10 *	8.19	0.369	0.206	513	9.42
M10-26 /	5.10	0.305	0.117	451	6.11	M12-11 *	7.76	0.371	0.205	536	8.98
M10-27 /	6.13	0.239	0.131	444	6.92	M12-12 *	8.33	0.356	0.214	530	9.50
M10-28 /	6.44	0.284	0.144	458	7.37	M12-13 *	8.38	0.361	0.211	519	9.57

Table 1. (continued)

Spot No.	ThO ₂	UO ₂	PbO	Age	RO ₂ *	Spot No.	ThO ₂	UO ₂	PbO	Age	RO ₂ *
M04-28 *	3.98	0.122	0.0939	504	4.38	M09-03 *	4.55	0.136	0.109	512	5.00
M04-29 /	6.90	0.189	0.132	415	7.52	M09-04 *	4.96	0.345	0.132	510	6.10
M04-30 /	6.52	0.159	0.127	425	7.04	M09-05 *	5.04	0.289	0.132	516	6.00
M04-31 /	5.56	0.164	0.118	454	6.10	M10-01 *	4.86	0.144	0.118	522	5.33
M04-31 /	6.00	0.167	0.125	450	6.55	M10-02	4.34	0.080	0.0900	460	4.60
M04-32 /	7.71	0.220	0.147	411	8.43	M10-03	5.13	0.241	0.118	470	5.92
M04-34 /	7.89	0.224	0.151	413	8.63	M10-04 /	4.47	0.116	0.0834	405	4.85
M04-35 /	7.74	0.205	0.156	437	8.41	M10-05	3.98	0.398	0.107	475	5.30
M04-36 /	4.78	0.083	0.0919	428	5.05	M10-06 /	4.35	0.317	0.104	455	5.39
M04-37 /	9.38	0.228	0.177	411	10.13	M11-02 /	4.32	0.084	0.0816	418	4.59
M04-38	4.45	0.087	0.0930	462	4.74	M11-03	4.09	0.228	0.0955	464	4.84
M05-01 /	4.33	0.180	0.0856	410	4.92	M11-04 *	4.15	0.202	0.108	528	4.82
M05-02 /	4.45	0.121	0.0879	427	4.85	M11-05 /	4.28	0.233	0.0957	447	5.04
M05-03 /	4.28	0.159	0.0936	458	4.80	M11-06 *	4.31	0.262	0.115	522	5.18
M05-04 /	4.73	0.109	0.0915	423	5.09	M11-07 *	3.69	0.138	0.0906	513	4.15
M05-05 /	4.19	0.123	0.0818	420	4.59	M11-08	4.12	0.064	0.0641	349	4.33
M05-06 /	4.54	0.344	0.108	448	5.67	M11-09	4.11	0.156	0.0939	478	4.62
M05-07 /	4.19	0.111	0.0840	434	4.55	M11-10 /	4.29	0.077	0.0794	412	4.54
M05-08 /	4.52	0.181	0.0997	458	5.12	M11-11 *	4.22	0.144	0.102	510	4.70
M05-09 /	4.64	0.268	0.103	439	5.52	M11-12	4.59	0.158	0.105	481	5.11
M05-10 /	4.22	0.335	0.0971	429	5.32	M11-13	3.94	0.096	0.0889	491	4.26
M05-11 /	4.31	0.287	0.0985	441	5.26	M11-14	3.88	0.127	0.0844	462	4.29
M05-12	4.62	0.167	0.101	461	5.17	M11-15 /	4.04	0.096	0.0765	414	4.36
M05-13	4.38	0.243	0.103	467	5.18	M12-01 /	5.88	0.208	0.126	451	6.56
M05-14 *	4.47	0.175	0.113	524	5.05	M12-02 /	5.10	0.091	0.105	457	5.40
M06-01 /	4.30	0.113	0.0894	450	4.67	M12-03 /	4.18	0.311	0.0993	449	5.20
M06-02 /	4.06	0.137	0.0826	431	4.51	M12-04	4.70	0.570	0.138	491	6.59
M06-03 /	5.18	0.141	0.105	439	5.64	M12-05	5.75	0.602	0.116	355	7.72
M06-04 /	4.30	0.127	0.0868	433	4.72	M12-06 /	4.45	0.143	0.0934	447	4.92
M06-05	5.56	0.165	0.123	472	6.11	M12-07 /	4.89	0.143	0.101	443	5.36
M06-06	4.45	0.094	0.0942	465	4.76	M12-08	4.64	0.111	0.101	475	5.00
M06-07 /	4.88	0.138	0.0982	433	5.33	M12-09	4.59	0.620	0.138	488	6.63
M06-08	4.54	0.108	0.0777	374	4.89	M12-10	5.57	0.687	0.162	487	7.84
M06-09	4.45	0.125	0.0987	477	4.86	M13-01 *	5.50	0.125	0.128	507	5.92
M06-10	4.42	0.121	0.101	491	4.82	M13-02 *	5.90	0.131	0.138	511	6.33
M06-11 /	5.98	0.153	0.124	451	6.48	M13-03 *	5.87	0.143	0.138	513	6.34
M07-02 /	5.84	0.158	0.109	402	6.36	M13-04 *	5.40	0.124	0.132	535	5.81
M07-03 /	5.28	0.157	0.0993	404	5.79	M13-05 *	4.74	0.121	0.113	515	5.14
M07-04 /	5.02	0.177	0.106	443	5.61	M13-06 *	4.24	0.116	0.101	511	4.63
M07-05	5.27	0.143	0.122	498	5.75	M13-07 *	5.44	0.130	0.126	506	5.87
M07-06 /	5.22	0.143	0.109	452	5.69	M13-08 *	5.59	0.133	0.137	532	6.03
M07-07	5.98	0.155	0.131	476	6.49	M13-09 *	5.39	0.174	0.134	528	5.97
M07-08 /	7.12	0.067	0.142	455	7.34	M13-10 *	5.30	0.189	0.133	527	5.93
M07-09 /	4.59	0.273	0.0991	425	5.49	M13-11 *	5.31	0.175	0.127	507	5.89
M07-10	4.85	0.080	0.0845	389	5.12	M13-12 *	6.74	0.169	0.167	538	7.31
M07-11	5.04	0.136	0.112	480	5.49	M13-13 *	6.96	0.168	0.166	518	7.52
M07-12	5.15	0.162	0.112	463	5.68	M13-14 /	6.16	0.143	0.127	451	6.63
M07-13	5.39	0.180	0.100	395	5.98	M13-15 /	5.19	0.136	0.104	436	5.64
M07-14	5.04	0.146	0.108	461	5.52	M13-16 /	5.47	0.151	0.115	454	5.97
M07-15	5.15	0.127	0.117	494	5.57	M13-17 *	7.44	0.223	0.187	538	8.18
M08-01 *	5.78	0.403	0.159	526	7.11	M13-18 *	8.03	0.207	0.194	522	8.72
M08-02 *	5.73	0.382	0.160	537	7.00	M13-19 *	5.52	0.131	0.131	516	5.95
M08-03 *	5.54	0.365	0.152	527	6.75	M13-20 *	6.42	0.144	0.152	519	6.90
M08-04 *	5.65	0.398	0.149	501	6.97	M13-21 *	4.33	0.100	0.108	543	4.66
M08-05 *	5.13	0.463	0.152	534	6.66	M13-22 *	5.13	0.115	0.123	524	5.51
M08-06 *	5.10	0.455	0.151	536	6.61	M13-23 *	5.51	0.138	0.136	533	5.97
M08-07 *	5.08	0.458	0.154	546	6.60	M13-24 *	5.32	0.124	0.130	533	5.73
M08-08 *	5.03	0.456	0.149	536	6.54	M13-25 *	4.82	0.117	0.114	515	5.21
M08-09 *	4.28	0.262	0.116	531	5.15	M13-26 *	4.99	0.131	0.124	538	5.43
M08-10 *	4.18	0.263	0.110	511	5.05						
M08-11 *	4.04	0.259	0.111	530	4.90						
M09-01 *	5.66	0.215	0.141	520	6.38						
M09-02 *	4.20	0.127	0.0995	506	4.62						

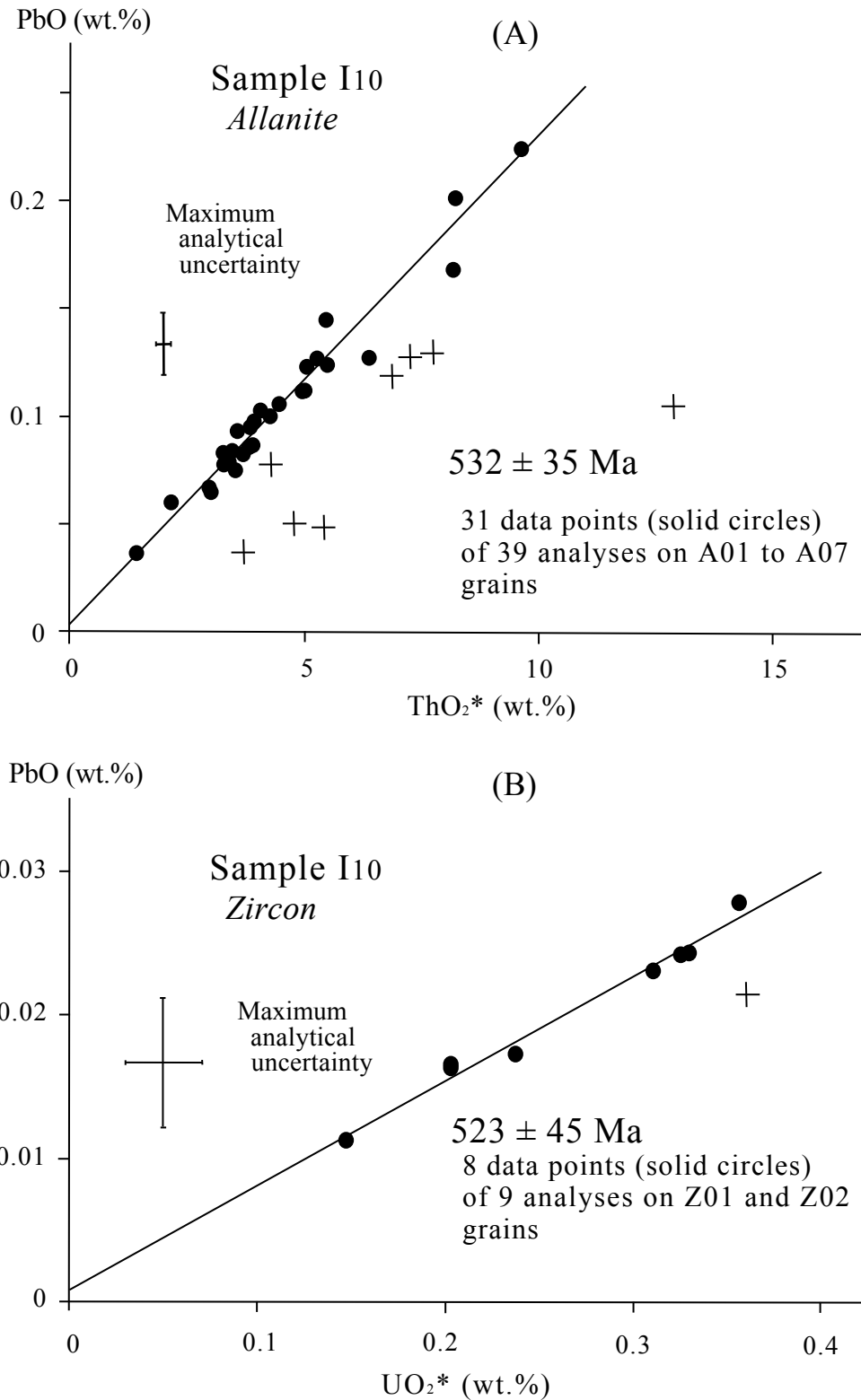


Fig. 3. A) PbO vs. ThO₂* plot of allanite grains from Sample I10. B) PbO vs. UO₂* plot of zircon grains from Sample I10. ThO₂* = the sum of the measured ThO₂ and ThO₂ equivalent of the measured UO₂; UO₂* = the sum of the measured UO₂ and UO₂ equivalent of the measured ThO₂. Error bars in the figures represent 2 σ maximum analytical uncertainty, and all errors are quoted at 2 σ .

A linear regression through the 31 data points defines an isochron of 532 ± 35 Ma age with an intercept of 0.0038 ± 0.0071 .

Zircon contains 0.061-0.270% ThO₂, 0.121-0.279% UO₂ and 0.011-0.0280% PbO. All data points, excepting one analysis on a clouded portion, were fitted to a linear regression, corresponding to an isochron of 523 ± 45 Ma with an intercept of 0.0008 ± 0.0019 (Fig. 3B). The CHIME allanite and zircon ages agree within the limit of analytical uncertainty.

Sample N₉: medium-grained porphyritic two-mica granite

A total of 213 spots on 14 monazite grains were analyzed. The ThO₂, UO₂ and PbO concentrations in monazite are 4.01-21.0, 0.160-0.611 and 0.103-0.518%, respectively. Grains M03, M04, M06,, M07, M08 and M09 rarely give apparent ages older than 460 Ma. The rest of the grains analyzed yielded apparent ages greater than 480 Ma. Data points for the older domains (>480 Ma, solid circles) and those for younger domains (<460 Ma, open circles) form separate arrays on the PbO-ThO₂* diagram (Fig. 4); 115 data points define an isochron of 530 ± 9 Ma with an intercept of -0.0032 ± 0.0034 , and 51 data points yield a 436 ± 13 Ma isochron with an intercept of 0.0039 ± 0.0056 .

Sample I₄: two-mica adamellite

A total of 216 spots on 13 monazite grains were analyzed. Six grains (M01, M02, M04, M08, M09 and M13) were from the fresh part of the sample; the other grains

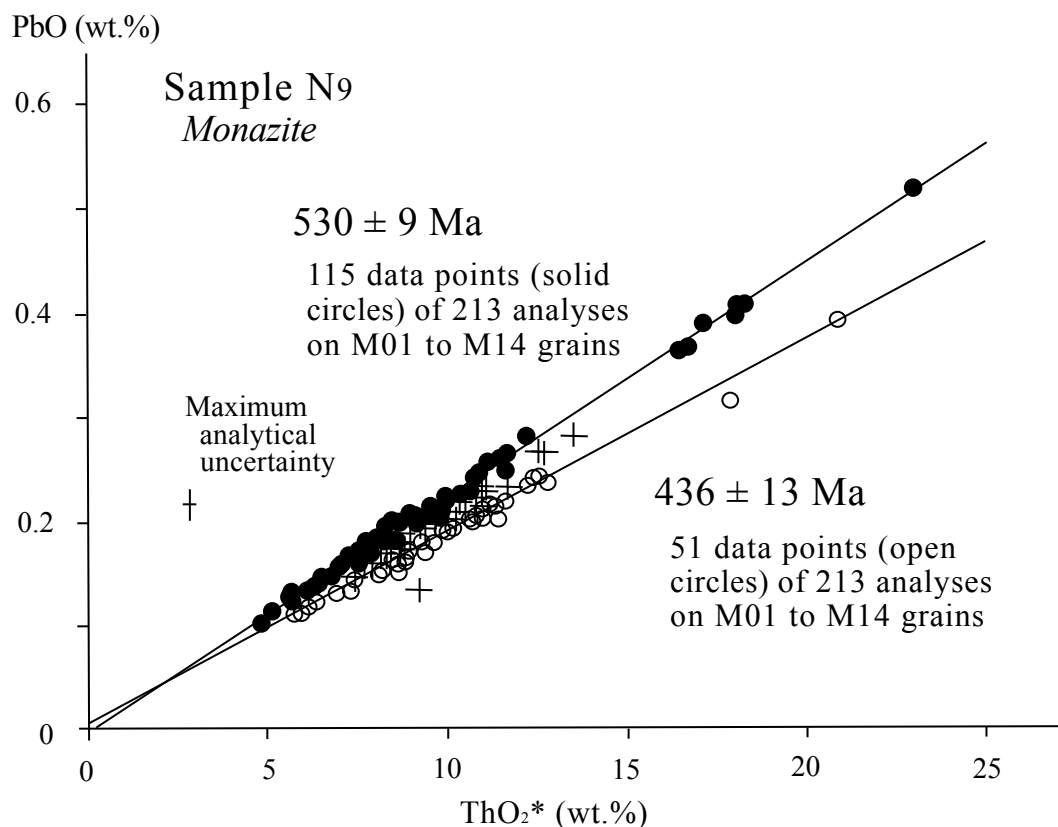


Fig. 4. PbO vs. ThO₂* plot of monazite grains from Sample N₉. Explanation for errors is the same as for Fig. 3.

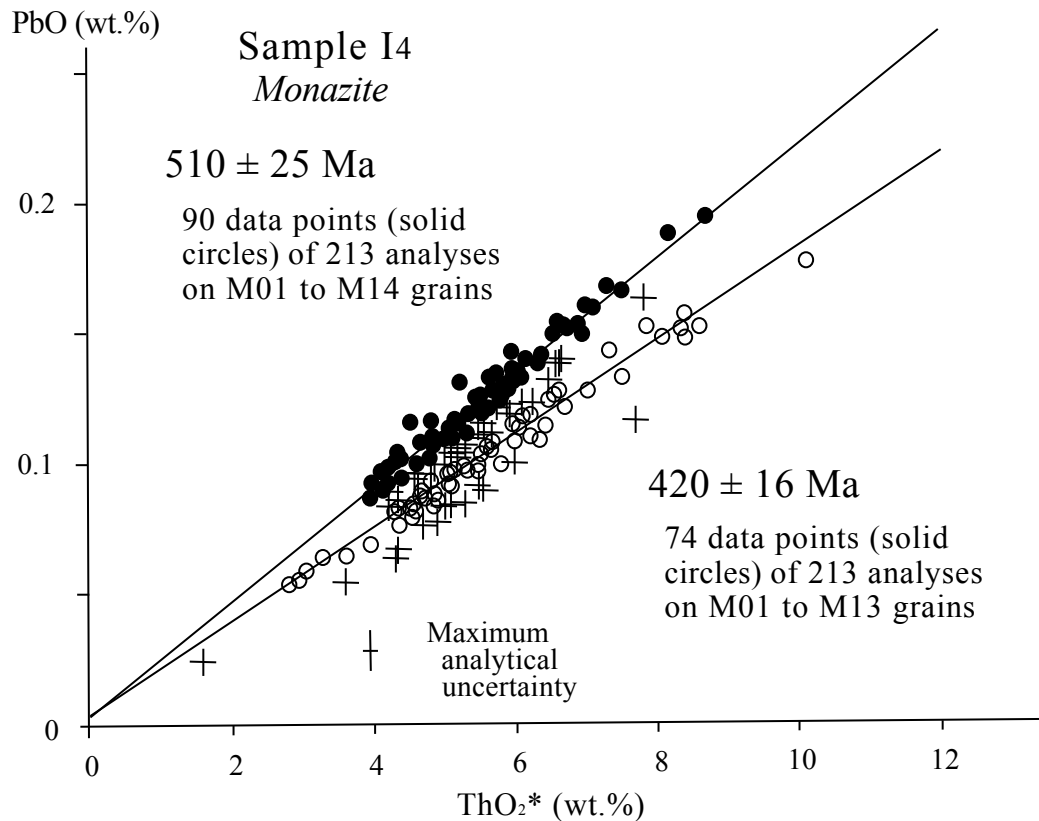


Fig. 5. PbO vs. ThO₂* plot of monazite grains from Sample I4. Explanation for errors is the same as for Fig. 3.

(M03, M05, M06, M07, M10, M11, and M12) were in or close to the altered patches. Monazite grains contain 1.54-9.38% ThO₂, 0.021-0.687% UO₂ and 0.0244-0.194% PbO, and no significant difference in the ThO₂ and UO₂ concentrations can be seen between grains from the fresh parts and the altered patches. Apparent ages differ significantly, however, between the two groups: monazites from the fresh parts are older than 500 Ma for most analyses; whereas monazites from the altered patches are usually younger than 450 Ma. Ninety data define an isochron of 510±25 Ma (intercept value = 0.0038±0.0060), and 74 data define an isochron of 420±16 Ma (intercept value = 0.0042±0.0040) (Fig. 5). Since the altered patches formed through hydrothermal events, permeation of fluids possibly caused the partial recrystallization of monazite at 420±16 Ma.

DISCUSSION

The CHIME ages are 532±35 Ma (allanite) and 523±45 Ma (zircon) for Sample I₁₀, 530±9 Ma and 436±13 Ma (monazite) for Sample N₉ and 510±25 Ma and 420±16 Ma (monazite) for Sample I₄. These dates, except the young two ages, just overlap within 2σ. We interpret the 532-510 Ma CHIME ages as dating the emplacement of granites in the Nkambe area. The younger 436±13 and 420±16 Ma ages are regarded as the time of late hydrothermal and/or thermal imprints. The foliated granites are essen-

tially synchronous with the regional metamorphism that produces the migmatitic gneiss, amphibolite and anatectic granite in the Nkambe area. As stated before, similar ca. 530 Ma granitoids are reported from Goutchoumi (525 Ma, Lasserre et al., 1981), Poli (520±20 Ma, Lasserre and Soba, 1976), Linte (521±19 Ma, Lasserre et al., 1981) and Lom (498±5 Ma, Lasserre and Soba, 1976) areas within the Central-Africa mobile zone of Cameroon (Fig. 1). An extensive metamorphic-plutonic event occurred in the Central African mobile zone at middle Cambrian time (530 Ma) rather than a thermal overprint.

Outside Cameroon, ca. 530 Ma ages were reported from granites in southeastern Nigeria (538±8 Ma for the Nassarawa Eggon Granite and 547±38 Ma for the Mkar-Gboko Granite, Umeji and Caen-Vachette, 1984). The 530 Ma episode in Cameroon and southeastern Nigeria was a metamorphic-plutonic episode caused possibly by collision of West Gondwana (Casting et al., 1993; Trompette, 1994). Although it has not been proven if the 530 Ma metamorphic belt in Cameroon is continuous to those in Madagascar, southern India and East Antarctica, the metamorphism and plutonism are contemporaneous in both West Africa and East Africa.

ACKNOWLEDGMENTS

We thank Mr. S. Yogo for providing excellent polished thin sections. Constructive reviews by Dr. K. Shibata of Nagoya Bunri University and Dr. D. Dunkley of Gamagori Natural History Museum have improved the manuscript.

REFERENCES

- Asami, M. Suzuki, K. and Adachi, M. (1996) Monazite ages by the chemical Th-U-total Pb isochron method for polytictic gneiss from the Eastern Sor Rondane Mountains, East Antarctica. *Proc. NIPR Symp. Antarct. Geosci.*, No. 9, 49-64.
- Asami, M. Suzuki, K. and Adachi, M. (1997) Th, U and Pb analytical data and CHIME dating of monazites from metamorphic rocks of the Rayner, Lutzow-Holm, Yamato-Belgica and Sor Rondane complexes, East Antarctica. *Proc. NIPR Symp. Antarct. Geosci.*, No. 10, 130-152.
- Bessoles, B. et Trompette, M. (1980) Géologie de l'Afrique: la chaîne panafricaine, <<zone mobile d'Afrique Centrale (parie sud) et zone mobile soudanaise>>. *Mém. BRGM, Orléans, France*, nx92 396p., 118 fig., 29 tabl., index, bibl. (20 p.).
- Bimdu, R.S. Suzuki, K., Yoshida, M. and Santosh, M. (1996) Pan-African tectonothermal events in East Gondwanaland: evidence from south Indian granulite using CHIME age dating. *Abst. 16th Symp. Antarct. Geosci. NIPR, Japan*, 66-67.
- Bimdu, R.S. Suzuki, K., Yoshida, M. and Santosh, M. (1998) The first report of CHIME monazite age from the South Indian granulite terrain. *Current Sci.*, **74**, 852-858.
- Cohen, L. and Snelling, N.J. (1966) The geochronology of equatorial Africa. *North-Holland Publ. Co., Amsterdam*, p195.
- Castaign, C., Triboulet, C., Feybesse, J.L. and Chevremont, P. (1993) Tectonometamorphic evolution of Ghana, Toga and Benin in the light of the Pan-African/Brasiliano orogeny. *Tectonophysics*, **218**, 323-342.
- Clifford, T.N. (1970) The structural framework of Africa. In: T.N. Clifford and I.G. Gass (ed) African magmatism and tectonics, 1, 1-26, Oliver and Boyd, Edinburgh.
- Ito, M. Suzuki, K. and Yogo, S. (1997) Cambrian granulite to upper amphibolite facies metamorphism of post-797 Ma sediments in Madagascar. *J. Earth Planet. Sci., Nagoya Univ.*, **44**, 89-102.

- Kennedy, W.Q. (1964) The structural differentiation of Africa in the Pan-African (± 500 million years) tectonic episode. *8th Ann. Rep. Res. Inst. Afr. Geol. (1962-1963) Leeds Univ., (UK)*, 48-49.
- Kröner, A. (1977) The Precambrian geotectonic evolution of Africa: plate accretion versus plate destruction. *Precambrian Res.*, **4**, 163-213.
- Lassere, M. (1966) Géochronologie du Cameroun. Rapport d'activité scientifique (1962 à 1966). Mesures d'âges absolus sur micas et sur roches totales. Technique et discussion des résultats. B.R.G.M. Paris Orleans, 74p.
- Lasserre, M. (1969) Cameroun: Examen des résultats géochronologiques obtenus depuis 1967. *Ann. Fac. Sci. Univ. Clermont-ferrand, Géol. Min.*, **41** (19), 29-31.
- Lasserre, M. et Bessoles, B. (1976) Géochronologie (Rb/Sr, K/Ar) des formations précambriennes du Cameroun méridional: Précision sur les limites du craton du Congo. *4e Réunion Annu. Sci. du la Tette, Paris, Soc. Géol. France*, p253.
- Lasserre, M. et Soba, D. (1976) Ages cambriens des granites de Nyibi et de Kongolo (Centre Est Cameroun). *C.R. Acad. Sc. Paris, 283, série D, 1696-1698*.
- Lasserre, M., Tempier, P. et Soba, D. (1981) Pétrographie et géochronologie Rb/Sr des granites cambriens de Goutchoumi et d'Anloa (Cameroun). *Bull. Soc. Géol. France, (7)*, **23**, 511-514.
- Peronne, (1969) Notice explicative sur la feuille Wum-Banyo. Direction des Mines et de la Géologie du Cameroun, 49p.
- Rocci, G. (1965) Ages absolus, histoire et structure de l'Ouest du bouclier africain. *C.R. Acad. Sci., Paris*, **258**, 2559-2562.
- Shiraishi, K., Ellis, D.J., Hiroi, Y., Fanning, C.M., Motoyoshi, Y. and Nakai, Y. (1994) Cambrian orogenic belt in East Antarctica and Sri Lanka: implications for Gondwana assembly. *Jour. Geol.*, **102**, 47-65.
- Suzuki, K. and Adachi, M. (1991a) Precambrian provenance and Silurian metamorphism of the Tsubonosawa paragneiss in the South Kitakami terrane, Northeast Japan, revealed by the chemical Th-U-total Pb isochron ages of monazite, zircon and xenotime. *Geochem. J.*, **25**, 357-376.
- Suzuki, K. and Adachi, M. (1991b) The chemical Th-U-total Pb isochron ages of zircon and monazite from the Gray Granite of the Hida Terrane, Japan. *J. Earth Sci., Nagoya Univ.*, **38**, 11-37.
- Suzuki, K. and Adachi, M. (1994) Middle Precambrian detrital monazite and zircon from the Hida gneiss on Oki-Dogo Island, Japan: their origin and implication for the correlation of basement gneiss of Southwest Japan and Korea. *Tectonophysics*, **235**, 277-292.
- Suzuki, K. and Adachi, M. (1998) Denuation history of the high T/P Ryoke metamorphic belt, southwest Japan: constraints from CHIME monazite ages of gneisses and granitoids. *J. Metamorphic Geol.*, **16**, 23-37.
- Suzuki, K., Adachi, M. and Tanaka, T. (1991) Middle Precambrian provenance of Jurassic sandstone in the Mino Terrane, central Japan: Th-U-total Pb evidence from an electron microprobe monazite study. *Sediment. Geol.*, **75**, 141-147.
- Suzuki, K., Adachi, M. and Kajizuka, I. (1994) Electron microprobe observations of Pb diffusion in metamorphosed detrital monazites. *Earth Planet. Sci. Lett.*, **128**, 391-405.
- Suzuki, K., Adachi, M., Kato, T. and Yogo, S. (1999) CHIME dating method and its application to the analysis of evolutionary history of orogenic belts. *Chikyukagaku (Geochemistry)*, **33**, 1-22.
- Tingey, R.J. (1991) The regional geology of Archaean and Proterozoic rocks in Antarctica. In R.J. Tingey (ed) *The geology of Antarctica*, 1-73, Oxford University Press, Oxford.
- Trompette, R. (1994) Geology of western Gondwana (200-500 Ma). A.A. Balkema, Rotterdam p350.
- Umeji, A.C. and Caen-Vachette, M. (1984) Geochronology of Pan-African Nassarawa Eggon and Mkar-Gboko granites, Southeast Nigeria. *Precambrian Res.*, **23**, 317-324.